Resonance Raman Spectra of Ferrochelatase Reveal Porphyrin Distortion upon Metal Binding

Milton E. Blackwood, Jr., Thomas S. Rush, III, Amy Medlock,‡ Harry A. Dailey,‡ and Thomas G. Spiro*

Contribution from the Department of Chemistry, Princeton University, Princeton, New Jersey 08544

Received May 19, 1997⊗

Abstract: Ferrochelatase catalyzes Fe^{2+} insertion into porphyrins, and is inhibited by Hg^{2+}. Resonance Raman spectra of mesoporphyrin IX show that binding to ferrochelatase restricts the conformation of the propionate side chains, but does not perturb the ring conformation. However, a pronounced perturbation is seen in the ternary complex with Hg^{2+}. Several additional RR bands are activated, including some arising from IR-active vibrations, establishing loss of an effective symmetry center. Out-of-plane modes appear in the low frequency region. The strongest of these bands, γ_5 and γ_6, correspond to pyrrole tilting vibrations, which are in the same symmetry class as a doming distortion of the porphyrin. All four pyrrole N atoms are pointing toward the same side of the porphyrin plane, a geometry expected to facilitate Fe^{2+} insertion. This distortion is proposed to result from occupation of a metal-binding site, proximate to the prophyrin, which promotes insertion of Fe^{2+}, while occupation by Hg^{2+} is inhibitory.

Introduction

Hemes are the prosthetic groups in a wide variety of proteins whose functions are as diverse as oxygen transport and activation, electron transfer, redox catalysis, and nitric oxide synthesis. Ferrochelatase is the terminal enzyme in heme biosynthesis and catalyzes insertion of ferrous iron into the porphyrin macrocycle.[1] The enzyme will also insert Co^{2+} and Zn^{2+} but is strongly inhibited by Hg^{2+}, Mn^{2+}, and Cd^{2+}, and weakly inhibited by Pb^{2+}.[2] Specificity of the porphyrin substrate is somewhat species dependent, but in all known cases only IX type isomers are effectively metalated.[2,3]

The proposed mechanism of ferrochelatase involves the distortion of the bound free-base porphyrin to expose the nitrogen lone pair electrons to the incoming metal ion.[3b,4] *N*-Alkylated porphyrins, which have structures that resemble this distortion,[5] strongly inhibit ferrochelatase, presumably by binding as transition state analogs.[6] Cochran and Schultz exploited this hypothesis to prepare antibodies specific for *N*-methylmesoporphyrin IX, which catalyze the insertion of divalent metals into planar porphyrins.[7]

We have used resonance Raman (RR) spectroscopy to probe the mechanism of yeast ferrochelatase (which lacks the iron−sulfur cluster found in mammalian ferrochelatase[8]). Spectra have been obtained of free-base mesoporphyrin IX, MPH_2
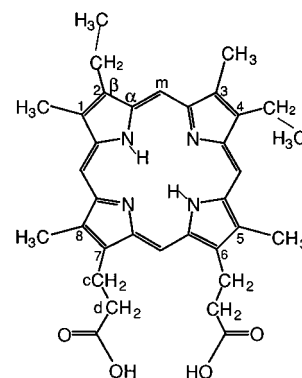

Figure 1. Atom labeling scheme for free-base mesoporphyrin IX.

(Figure 1), bound to yeast ferrochelatase in the absence and presence of Hg^{2+}, and in solution. The data indicate that porphyrin binding to ferrochelatase alone is not enough to cause significant distortion of the macrocycle. However, in the presence of Hg^{2+} the structure of the bound porphyrin is significantly altered, as determined by the activation of many new vibrational features in its RR spectrum.

Experimental Section

Sample Preparation. The purification of yeast ferrochelatase is described in detail elsewhere.[9] Mesoporphyrin IX was purchased from Midcentury Chemicals (Posen, IL). Binding of mesoporphyrin to ferrochelatase was monitored by fluorescence anisotropy measurements[10] performed on a Perkin Elmer LS50 luminescence spectrometer. Protein RR spectra were obtained on solutions (pH 8.0 Tris buffer) that were 50 μM in porphyrin and 55 μM ferrochelatase, the protein being kept in slight excess to minimize unbound porphyrin. For the ternary complex, a slight excess of $HgCl_2$ was added. The spectrum

(1) Jordan, P. M. *Curr. Opin. Struct. Biol.* **1994,** *4,* 902−911.

(2) Dailey, H. A. In *Biosynthesis of Heme and Chlorophylls*; Dailey, H. A., Ed.; McGraw-Hill Publishing Company: New York, 1990; 123−161.

(3) (a) Dailey, H. A.; Jones, C. S.; Karr, S. W. *Biochim. Biphys. Acta* **1989,** *999,* 7−11. (b) Dailey, H. A. In *Mechanisms of Metallocenter Assembly*; Hausinger, R. P., Eichorn, G. C., Marzilli, C. G., Eds.; VCH: New York, 1996; pp 77−89.

(4) Lavallee, D. K. In *Mechanistic Principles of Enzyme Activity*; Liebman, J. F., Greeberg, A., Eds.; VCH: New York, 1988; pp 279−314.

(5) Sparks, L. D.; Chamberlain, J. R.; Hsu, P.; Ondrias, M. R.; Swanson, B. A.; Ortiz de Montellano, P. R.; Shelnutt, J. A. *Inorg. Chem.* **1993,** *32,* 3153−3161.

(6) Dailey, H. A.; Fleming, J. E. *J. Biol. Chem.* **1983,** *258 (11),* 453.

(7) Cochran, A. G.; Schultz, P. G. *Science* **1990,** *249,* 781−783.

(8) (a) Dailey, H. A.; Finnegan, M. G.; Johnson, M. K. *Biochemistry* **1994,** *33,* 403−407. (b) Ferreira G. C.; Franco, R.; Lloyd, S. G.; Pereira, A. S.; Moura, I.; Moura, J. J. G.; Huynh, B. H. *J. Biol. Chem.* **1994,** *269 (10),* 7062−7065. (c) Crouse, B. R.; Sellers, V. M.; Finnegan, M. G.; Dailey, H. A.; Johnson, M. K. *Biochem*istry **1996,** *35,* 16222−16229.

(9) Sellers, V. M.; Dailey, H. A. *Methods Enzymol.* **1997,** *281,* 378−387.

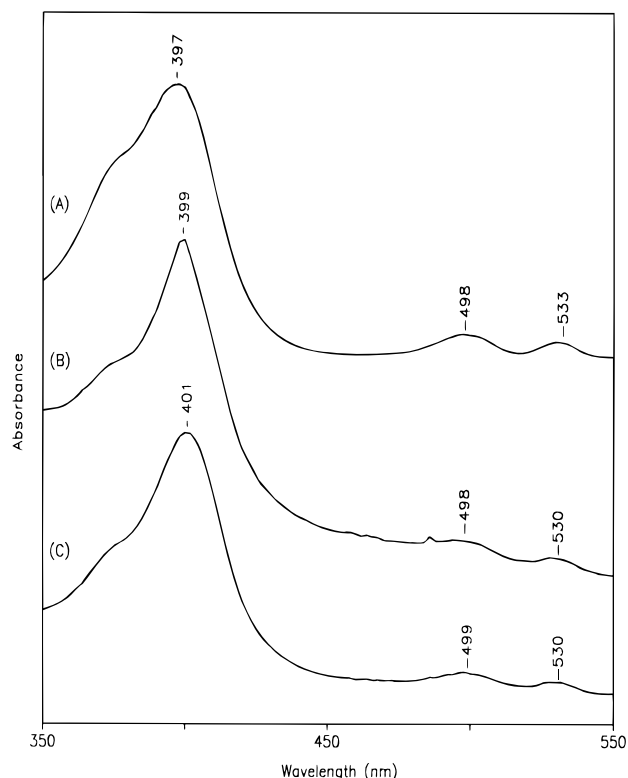(10) Dailey, H. A. *Biochem*istry **1985,** *24,* 1287−1291.

Figure 2. Electronic absorption spectrum of mesoporphyrin IX: (A) in solution; (B) bound to ferrochelatase in the absence of Hg^{2+}; and (C) bound to ferrochelatase in the presence of Hg^{2+}.

Figure 3. Excited resonance Raman spectra (407 nm) of mesoporphyrin IX: (A) in solution; (B) bound to ferrochelatase in the absence of Hg^{2+}; and (C) bound to ferrochelatase in the presence of Hg^{2+}.

of free-base mesoporphyrin was obtained in pH 6.8 Tris buffer at a concentration of 300 μM. All solutions were degassed prior to Raman measurements.

Spectroscopy. Electronic absorption spectra were measured with a Hewlett Packard Diode Array 8451A UV–vis spectrophotometer. RR spectra were obtained in spinning NMR tubes utilizing 135° backscattering geometry and a triple-stage spectrograph equipped with a diode array detector (Princeton Instruments). The 407-nm line of a Kr^+ laser (Coherent Innova K100) was selected as the excitation source, as this wavelength is in resonance with the Soret absorption band of mesoporphyrin IX. The laser power at the sample was approximately 15 mW, and spectral acquisition times were 10 min. Sample integrity was monitored by measuring the electronic absorption spectra before and after each Raman experiment. The spectral data were processed with the Labcalc software package (Galactic Industries Co).

Results

The electronic absorption spectrum of mesoporphyrin IX is modified slightly upon binding to ferrochelatase, and upon formation of the ternary complex with Hg^{2+} (Figure 2). The Soret band alters shape and shifts progressively to longer wavelengths. While out-of-plane distortions of the porphyrin are known to produce Soret red shifts,[11,12] changes are also expected from dielectric and electrostatic influences of the protein. To obtain structural information, we turn to RR spectroscopy, which has been useful in characterizing structural effects in heme proteins.[13–16]

Most detailed vibrational studies of porphyrins have focused on metalated complexes,[17–24] but free-base porphyrins have also been investigated.[25–27] Although replacement of the central metal with two protons reduces the idealized symmetry of the conjugated π-system from D_{4h} to D_{2h}, Soret-excited RR spectra of free-base porphyrins have enhancement patterns similar to those of the parent metalloporphyrin.[25,26] In addition, Perng and Bocian demonstrated that RR features of free-base octa-ethylporphyrin (H_2OEP) could be correlated straightforwardly with those of metallo-OEPs using isotope labeling and depolarization ratio measurements.[26] We assign the RR spectra of free-base mesoporphyrin in the same manner (Figures 3 and 4, Table 1). The RR spectrum of mesoporphyrin bound to ferrochelatase is nearly identical with that of the protein-free mesoporphyrin (Figures 3 and 4). The bands are unaltered in position or relative intensity, except that the 988-cm^{-1} band is sharpened and stronger, and a new band is seen at 1592 cm^{-1}, which is assigned to an additional porphyrin skeletal vibration, ν_2.

(11) Shelnutt, J. A.; Medforth, C. J.; Berber, M. D.; Barkigia, K. M.; Smith, K. M. *J. Am. Chem. Soc.* **1991**, *113*, 4077–4087.

(12) Shelnutt, J. A.; Majunder, S. A.; Sparks, L. D.; Hobbs, J. D.; Medforth, C. J.; Senge, M. O.; Smith, K. M.; Miura, M.; Luo, L.; Quirke, J. M. E. *J. Raman Spectrosc.* **1992**, *23*, 523–529.

(13) Spiro, T. G. In *Iron Porphyrins Part B*; Lever, A. B. P., Gray, H. B., Eds.; Addison-Wesley: Reading MA, 1983; pp 89–159.

(14) Spiro, T. G. *Adv. Pro. Chem.* **1985**, *37*, 111–159.

(15) Kitagawa, T.; Ozaki, Y. *Struct. Bonding* **1987**, *64*, 71–114.

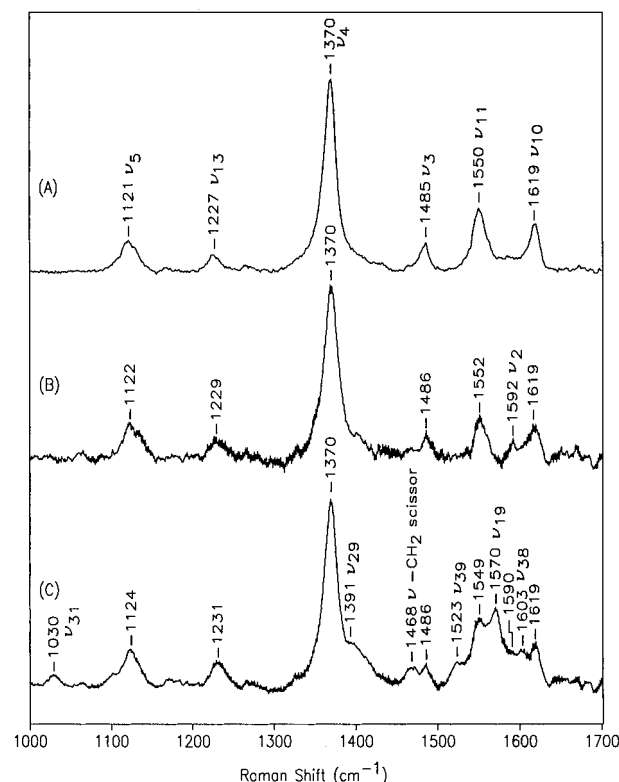(16) Procyk, A. D.; Bocian, D. F. *Annu. Rev. Phys. Chem.* **1992**, *43*, 465–496.

(17) Abe, M.; Kitagawa, T.; Kyogoku, Y. *Chem. Phys.* **1978**, *69*, 4526–4534.

(18) Li, X.-Y.; Czernuszewicz, R. S.; Kincaid, J. R.; Spiro, T. G. *J. Am. Chem. Soc.* **1989**, *111*, 7012–7023.

(19) Czernuszewicz, R. S.; Li, X.-Y.; Spiro, T. G. *J. Am. Chem. Soc.* **1989**, *111*, 7024–7031.

(20) Li, X.-Y.; Czernuszewicz, R. S.; Kincaid, J. R.; Stein, P.; Spiro, T. G. *J. Am. Chem. Soc.* **1990**, *94*, 47–61.

(21) Li, X.-Y.; Czernuszewicz, R. S.; Kincaid, J. R.; Su, Y. O.; Spiro, T. G. *J. Phys. Chem.* **1990**, *94*, 31–47.

(22) Piffat, C.; Melamed, D.; Spiro, T. G. *J. Phys. Chem.* **1993**, *97*, 7441–7450.

(23) Hu, S.; Mukherjee, A.; Piffat, C.; Mak, R. S.; Li, X.-Y.; Spiro, T. G. *Biospectroscopy* **1995**, *1*, 395–412.

(24) Hu, S.; Smith, K. M.; Spiro, T. G. *J. Am. Chem. Soc.* **1996**, *118*, 12638–12646.

(25) Sato, S.; Someda-Asano, M.; Kitagawa, T. *Chem. Phys. Lett.* **1992**, *189*, 443–447.

(26) Perng, J.-H.; Bocian, D. F. *J. Phys. Chem.* **1992**, *96*, 4804–4811.

(27) Li, X.-Y.; Zgierski, M. Z. *J. Phys. Chem.* **1991**, *95*, 4268–4287.
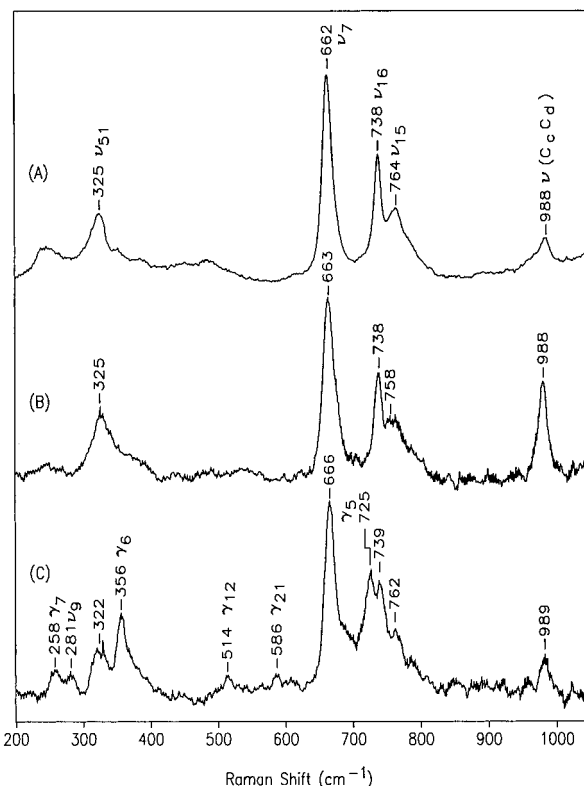
Figure 4. Same as Figure 3 except the low-frequency regions of the spectra are shown.

Table 1. Resonance Raman Frequencies (cm^{-1}) and Assignments for Free-Base Mesoporphyrin IX[a]

mode[b]	Meso. IX[c]	Meso. IX[d]	Meso. IX[e]	Symmetry[f]
ν_{10} (C$_\alpha$C$_m$)$_{asym}$	1619	1619	1619	A$_g$
ν_{38} (C$_\beta$C$_\beta$)	*	*	1603	B$_{2u}$/B$_{3u}$
ν_2 (C$_\beta$C$_\beta$)	*	1592	1590	A$_g$
ν_{19} (C$_\alpha$C$_m$)$_{asym}$	*	*	1570	B$_{1g}$
ν_{11} (C$_\beta$C$_\beta$)	1550	1552	1549	A$_g$
ν_{39} (C$_\alpha$C$_m$)$_{sym}$	*	*	1523	B$_{2u}$/B$_{3u}$
ν_3 (C$_\alpha$C$_m$)$_{asym}$	1485	1486	1486	A$_g$
-CH$_2$ scissor	*	*	1468	A$_g$
ν_{29} (pyr quarter ring)	*	*	1394	B$_{1g}$
ν_4 (pyr half ring)$_{sym}$	1370	1370	1370	A$_g$
ν_{13} (C$_m$H)	1227	1229	1231	A$_g$
ν_5 (C$_\beta$C$_1$)$_{sym}$	1121	1122	1124	A$_g$
ν_{31} (C$_\beta$C$_1$)$_{asym}$	*	*	1030	B$_{1g}$
ν(C$_c$C$_d$)	988	988	989	—
ν_{15} (pyr breathing)	764	760	762	A$_g$
ν_{16} (pyr deform)$_{sym}$	738	738	739	A$_g$
γ_5 (pyr fold)$_{sym}$	*	*	725	B$_{1u}$
ν_7 (pyr deform)$_{sym}$	662	663	666	A$_g$
γ_{21} (pyr fold)$_{sym}$	*	*	586	B$_{2g}$/B$_{3g}$
γ_{12} (pyr swivel)	*	*	514	A$_u$
γ_6 (pyr tilt)	*	*	356	B$_{1u}$
ν_8 (C$_\beta$C$_1$)$_{bend}$	325	325	322	A$_g$
ν_9 (C$_\beta$C$_1$)$_{bend}$	*	*	281	A$_g$
γ_7 (C$_\alpha$C$_m$)	*	*	258	B$_{1u}$

[a] An asterisk indicates not observed. [b] Based on NiOEP normal mode description (refs 18 and 20). [c] In solution. [d] Bound to ferrochelatase in the absence of Hg^{2+}. [e] Bound to ferrochelatase in the presence of Hg^{2+}. [f] Based on symmetry correlation of vibrational modes in $\textbf{D}_{4h}$ metalloporphyrins with $\textbf{D}_{2h}$ free-base mesoporphyrin IX.

Many new bands are seen for the ternary complex with Hg^{2+} (Figures 3 and 4). They can likewise be assigned to porphyrin vibrations by reference to the RR spectrum of ferrocytochrome c in which most of the heme modes are activated[28] (see Table 1). These include several out-of-plane modes (γ_5, γ_{12}, and γ_{21})

(28) Hu, S.; Morris, I. K.; Singh, J. P.; Smith, K. M.; Spiro, T. G. *J. Am. Chem. Soc.* **1993**, *115*, 12446−12458.

in the low-frequency region (Figure 4), and additional substituent (−CH$_2$ scissor) and skeletal modes (ν_{38}, ν_{19}, and ν_{39}). The ν_{39} (1523 cm^{-1}) mode is not observed in ferrocytochrome c, but has been identified in the IR spectrum of NiOEP (1501 cm^{-1}).[18] (An alternative assignment to the ν_{15} (762 cm^{-1}) overtone, which has been detected in the Q-band excited spectrum of ferrocytochrome c,[28] can be ruled out because the 1523-cm^{-1} intensity is greater than the 762-cm^{-1} intensity.) Two other modes enhanced in the presence of Hg^{2+} are assigned to out-of-plane modes detected in the ruffled form of NiOEP based on similar vibrational frequencies:[18,19] the 356-cm^{-1} peak to γ_6, a pyrrole tilting mode, and the 258-cm^{-1} feature to γ_7, a wagging mode of the methine bridges. γ_6 is seen at 351 cm^{-1} in the ruffled form of NiOEP while γ_7 is seen at 254 cm^{-1}.[18] ν_{50} is also detected at 360 cm^{-1} in the Soret-excited spectrum of ferrocytochrome c, but this mode is primarily a metal−nitrogen stretching mode and is not expected in the RR spectrum of free-base mesoporphyrin.[28]

We considered the possibility that the numerous RR bands in the ternary Hg^{2+} complex might reflect a mixture of bound and unbound mesoporphyrin, perhaps due to anticooperativity between mesoporphyrin and Hg^{2+} binding. However, the fluorescence anisotropy is nearly identical ($\pm 5\%$) for the mesoporphyrin/ferrochelatase solution in the absence and presence of Hg^{2+} showing no mesoporphyrin displacement.[10] In addition, the Hg^{2+} was found to prevent Fe^{2+} insertion into the mesoporphyrin, precluding a mixture of active and inhibited sites. The red shift in the Soret maximum upon Hg^{2+} binding (Figure 2) results in stronger RR scattering with 407-nm excitation as can be seen in the higher signal-to-noise ratio for the Hg^{2+} ternary complex (Figures 3 and 4).

Discussion

The RR spectrum of MPH$_2$, which closely resembles that of H$_2$OEP,[24] is readily assignable with reference to the porphyrin skeletal modes of NiOEP[20] and other β-substituted metalloporphyrins[23] of effective $\textbf{D}_{4h}$ symmetry. With excitation in the Soret absorption band, resonance enhancement is expected mainly for totally symmetric modes,[29] and the MPH$_2$ enhancement pattern is that expected upon symmetry reduction from $\textbf{D}_{4h}$ to $\textbf{D}_{2h}$ in the diprotonated free-base. The $\textbf{D}_{4h}$ symmetry classes A$_{1g}$ and B$_{1g}$ both correlate with the totally symmetric class, A$_g$, in the $\textbf{D}_{2h}$ point group, and they account for all but one of the RR bands of MPH$_2$ in solution (Figures 3 and 4): ν_{3-8}-A$_{1g}$ and ν_{10-16}-B$_{1g}$. The one additional band, at 988 cm^{-1}, is assigned to a C$_c$C$_d$ stretching mode of the propionate substituents (Figure 1) on the basis of isotope labeling studies in myoglobin.[24] Its enhancement is believed to arise from a hyperconjugation effect of the substituents:[20] In other respects the substituents do not influence the RR pattern, even though they reduce the formal symmetry of the molecule.

The bands which are additionally enhanced in the Hg^{2+}−ferrochelatase−MPH$_2$ ternary complex mainly arise from modes which are nontotally symmetric in the $\textbf{D}_{2h}$ point group. They include B$_g$ in-plane skeletal modes, deriving from the $\textbf{D}_{4h}$ skeletal classes B$_{2g}$ (ν_{29}, ν_{31}) and A$_{2g}$ (ν_{19}), and B$_{2u}$/B$_{3u}$ modes, deriving from the infrared-active E$_u$ modes ν_{38} and ν_{39}. In addition, several bands are activated in the low-frequency region (Figure 4) which arise from out-of-plane vibrations: γ_5, γ_6, γ_7, γ_{12}, and γ_{21}. This pattern signals a significant reduction in the porphyrin symmetry from $\textbf{D}_{2h}$. The E$_u$ mode activation requires loss of the effective symmetry center, and the B$_g$ mode activation implies a loss of the 2-fold rotation axes so that these

(29) Spiro, T. G.; Li, X.-Y. in *Biological Applications of Raman Spectroscopy*; Spiro, T. G., Ed.; Wiley: New York, 1988; Vol. 3.
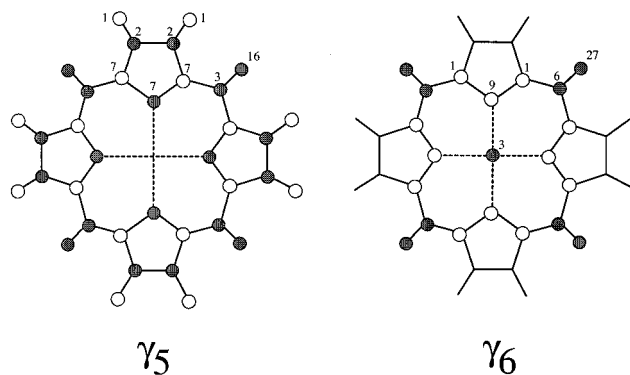
Figure 5. Illustration of the eigenvectors for γ_5 and γ_6 in NiOEP, adopted from ref 18. The direction is indicated by open (up) and filled (down) circles, and the numbers give the relative displacement of each atom.

Figure 6. ν_{10} and γ_{12} regions of ferricytochrome c RR spectra (406.7 nm excitation): (A) pH 7.0, 100 mM phosphate buffer; (B) pH 7.0, 500 mM imidazole, 100 mM phosphate buffer; and (C) pH 7.0, 4.0 M GuHCl, 100 mM phosphate buffer.

modes become totally symmetric. Most significant is the activation of the out-of-plane modes, since this provides a direct indication of a static out-of-plane distortion of the molecule.

Such distortions have been analyzed in heme proteins by Shelnutt and co-workers,[30] who decomposed them into linear combinations of out-of-plane normal coordinates. A static distortion is expected to produce RR activation of additional modes in the same symmetry class as the distortion coordinate, since the excited state will be displaced along modes which are totally symmetric in the point group of the distorted molecule. For example, cytochrome c has a ruffled heme,[31] and the main distortion coordinate[30] is the B_{1u} mode γ_{14}, which leads directly to the ruffled geometry. This mode is calculated for NiOEP[18] to be at ~45 cm^{-1}, too low a frequency to be detected in RR spectra. However, activation is observed for γ_{12} [514 cm^{-1}], another out-of-plane mode in the B_{1u} symmetry class. This activation disappears when cytochrome c is unfolded in acid, signalling relaxation of the heme distortion.[32]

For the Hg^{2+}−ferrochelatase−MPH_2 complex the γ_5 and γ_6 modes become activated, and indeed are stronger than many of the in-plane modes. These modes are in the A_{2u} symmetry class, in which the pyrrole N atoms all move in the same direction [see eigenvectors in Figure 5].[18] The lowest frequency mode of this symmetry class is γ_9 [predicted at ~32 cm^{-1}], which produces a domed conformation of the porphyrin.[30,33] This is just the sort of distortion that would assist in coordination of metal ions. Thus the RR spectrum of the ternary complex provides strong evidence supporting the idea that the enzyme distorts the porphyrin in a manner that lowers the activation energy for metal ion insertion.

Out-of-plane porphyrin distortions were originally examined in the context of NiOEP, which crystallizes in both planar and ruffled allotropes.[18,19,34] The ruffling in this case stems from the Ni^{2+} ion being smaller than the central cavity of a planar porphyrin;[35] ruffling allows the Ni−N bonds to shorten, at the expense of the delocalization energy, which is maximized in
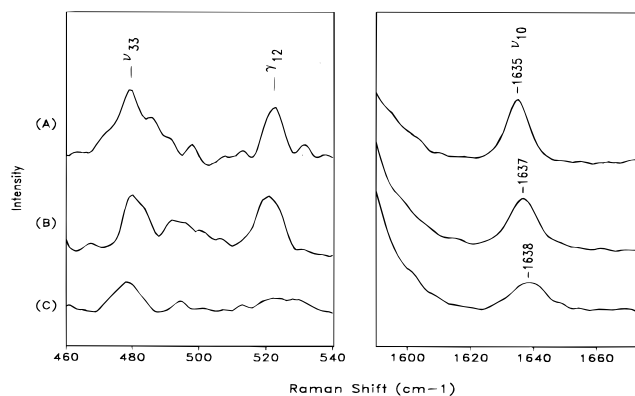
the planar structure. The alternative conformations are close enough in energy to be differentially stabilized by alternative crystal packing arrangements. In the ruffled form, out-of-plane modes are activated in the RR spectrum, permitting their assignments through isotope labeling.[18] In addition, however, several skeletal modes are shifted, relative to the planar form, as a result of bonding changes in the ring.[36] Even larger shifts are seen in sterically encumbered porphyrins, such as OETPP,[22,38−40] in which nonbonded repulsion of the C_β and C_m substituents enforces large distortions from planarity.[37] Such porphyrins have been studied extensively, as model systems for the distortions imposed by proteins on many biological tetrapyrrolic chromophores.[38] Attention has been focussed particularly on the highest frequency RR band, ν_{10}, as an indicator of distortion.[39−41] This band is lowered by 21 cm^{-1} between the planar and ruffled forms of NiOEP.[19]

However, distortion does not necessarily produce significant skeletal mode frequency shifts in porphyrins−doming or otherwise. As an example, we show in Figure 6 that the ν_{10} band of ferricytochrome c shifts up 2 cm^{-1} when 0.5 M imidazole [ImH] is added to the solution, while the addition of 4 M guanidine hydrochloride [GuHCl], a denaturant known to unfold the protein and leave a non-native bis-histidine-ligated relaxed heme,[42] only shifts the frequency up by 3 cm^{-1}. The γ_{12} band is seen to disappear in 4 M GuHCl, establishing relaxation of the heme geometry, while it remains in the 0.5 M ImH spectrum. Thus 2 cm^{-1} out of the 3 cm^{-1} denaturation-induced shift could be attributable to the change in coordination [ImH replacing the native methionine ligand[42,43]] and the remaining 1 cm^{-1} to relaxation of the heme distortion. We note that a slightly larger shift, 4 cm^{-1}, was observed by Desbois and co-workers between different ligation states of microperoxidase, a truncated form of cytochrome c.[41] This shift was

(30) Jentzen, W.; Song, X.-Z.; Shelnutt, J. A. *J. Phys. Chem. B* **1997**, *101*, 1684−1699.

(31) (a) Louie, G.; Brayer, G. D. *J. Mol. Biol.* **1990**, *214*, 527−555. (b) Berghuis, A. M.; Brayer, G. D. *J. Mol. Biol.* **1992**, *223*, 959−976.

(32) Jordan, T.; Eads, J. C; Spiro, T. G. *Protein Sci.* **1995**, *4*, 716−728.

(33) Jentzen, W.; Simpson, M. C.; Hobbs, J. D.; Song, X.; Ema, T.; Nelson, N. Y.; Medforth, C. J.; Smith, K. M.; Veyrat, M.; Mazzanti, M.; Ramasseul, R.; Marchon, J.-C.; Takeuchi, T.; Goddard, W. A., III; Shelnutt, J. A. *J. Am. Chem. Soc.* **1995**, *117*, 11085−11097.

(34) Brennan, T. D.; Scheidt, W. R.; Shelnutt, J. A. *J. Am. Chem. Soc.* **1988**, *110*, 3919.

(35) Hoard, J. L. In *Porphyrins and Metalloporphyrins*; Smith, K. M., Ed.; Elsevier: Amsterdam, 1975; Chapter 8.

(36) Prendergast, K.; Spiro, T. G. *J. Am. Chem. Soc.* **1992**, *114*, 3793−3801.

(37) Barkigia, K. M.; Berber, M. D.; Fajer, J.; Medforth, C. J.; Renner, M. W.; Smith, K. M. *J. Am. Chem. Soc.* **1990**, *112*, 8851−8857.

(38) Stichternath, A.; Schweitzer-Stenner R.; Dreybrodt, W.; Mak. R. S. W.; Li, X.-Y.; Sparks, L. D.; Shelnutt, J. A.; Medforth, C. J.; Smith, K. M. *J. Phys. Chem.* **1993**, *37*, 3701−3708.

(39) Shelnutt, J. A.; Majumder, S. A.; Sparks, L. D.; Hobbs, J. D.; Medforth, C. J.; Senge, M. O.; Smith, K. M.; Miura, M.; Luo, L.; Quirke, J. M. E. *J. Raman Spectrosc.* **1992**, *23*, 523−529.

(40) Shelnutt, J. A.; Medforth, C. J.; Berber, M. D.; Barkigia, K. M.; Smith, K. M. *J. Am. Chem. Soc.* **1991**, *113*, 4077−4087.

(41) Othman, S.; Le Lirzin, A.; Desbois, A. *Biochemistry* **1994**, *33*, 15437−15448.

(42) Elove, G. A.; Bhuyan, A. K.; Roder, H. *Biochemistry* **1994**, *33*, 6925−6935.

(43) (a) Babul, J.; Stellwagen, E. *Biopolymers* **1971**, *10*, 2359−2361. (b) Babul, J.; Stellwagen, E. *Biochemistry* **1972**, *11*, 1195−1200.

cited as evidence that the heme relaxes once it becomes 6-coordinate with two exogenous His ligands. However, some of this shift might be due to the ligation change *per se.* In any event, neither this 4-cm^{-1} shift nor the 3-cm^{-1} shift associated with cytochrome *c* denaturation is significant compared to the 21-cm^{-1} difference between planar and ruffled forms of NiOEP. This result is consistent with the empirical finding of Shelnutt and co-workers that skeletal mode shifts become significant only for large distortions (> 20°) in the ruffling angle.[33] The average ruffling angle is smaller than this (∼15°) for cytochrome *c*, but larger (∼30°) for the ruffled form of NiOEP. Thus the skeletal frequencies may not be sensitive to moderate degrees of ruffling.

The distortions that are evident in the RR spectrum of the ternary complex with Hg^{2+} are not seen for the binary complex of MPH$_2$ with ferrochelatase. The spectrum of the binary complex is almost identical with that of MPH$_2$ in solution. Only one additional RR band is activated, at 1592 cm^{-1}, and is assigned to ν_2. This is a totally symmetric skeletal mode, which is not enhanced in MPH$_2$ but becomes weakly enhanced upon ferrochelatase binding. This effect could arise from electrostatic fields of protein residues, which could influence the excited state potential and alter the enhancement pattern. One other notable effect of ferrochelatase binding is a sharpening and intensification of the 988-cm^{-1} band (Figure 3), assigned to the propionate C$_c$C$_d$ stretch. This band is broad in the solution spectrum, probably reflecting a distribution of orientations of the propionate groups relative to the porphyrin. The sharpening of this band upon ferrochelatase binding likely reflects the adoption of fixed propionate orientations at the binding site. This would be consistent with the proposal that propionates may be involved in the macrocycle alignment via interactions with an enzyme arginyl residue(s).[2,44] Intriguingly, the band broadens again in the ternary complex with Hg^{2+}. Possibly the propionates become unmoored from the docking sites when the porphyrin undergoes distortion.

What is the significance of seeing the porphyrin distortion only in the ternary complex with Hg^{2+}? We propose that the Hg^{2+} binds to a site adjacent to the porphyrin that is designed for Fe^{2+}, resulting in inhibition of the enzyme (Figure 6). Occupation of the metal site does, however, activate the porphyrin by distorting its geometry along the reaction coordinate for metal insertion. Hg^{2+} does not insert into the porphyrin, presumably because its coordination geometry differs enough from Fe^{2+} to misalign the metal with respect to the

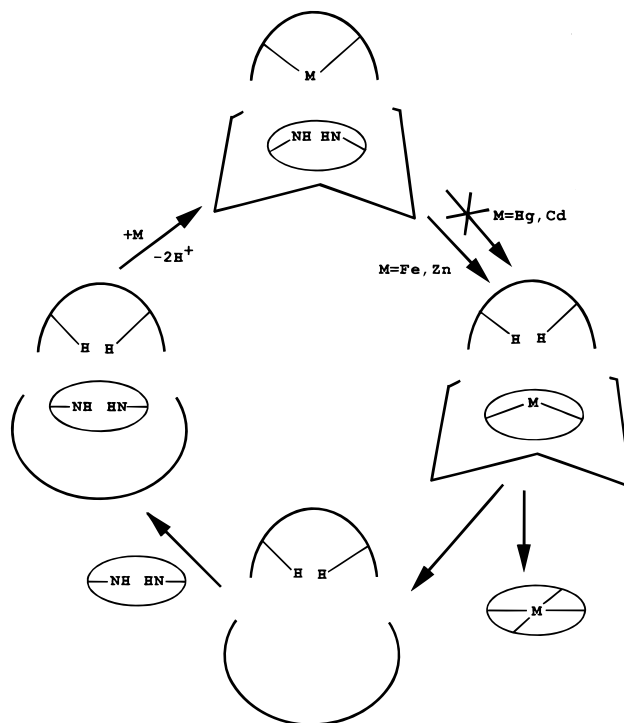(44) Dailey, H. A.; Fleming, J. E. *J. Biol. Chem.* **1986**, *261*, 7902−7905.

Figure 7. Proposed mechanism for the insertion of a metal into a free-base porphyrin by ferrochelatase.

porphyrin; Zn^{2+}, however, does insert. In the absence of metal, MPH$_2$ binds to ferrochelatase but is not distorted. Coupling of the distortion to metal site occupancy provides a strong element of control by ensuring the porphyrin is only activated when the metal is prepared for insertion. It may also assist in the dissociation reaction by relaxing the porphyrin site once the metal has been inserted and its binding site is vacant. Thus a cyclic mechanism is envisioned (Figure 7) in which both the porphyrin and the metal must bind in order to convert binding energy to porphyrin distortion along the reaction coordinate.